ROZPRAWY INŻYNIERSKIE • ENGINEERING TRANSACTIONS • 31, 3, 361—378, 1983
Polska Akademia Nauk • Instytut Podstawowych Problemów Techniki

PONDING INSTABILITY OF AIR-SUPPORTED ELASTIC SPHERICAL MEMBRANES (*)

G. AHMADI (NEW YORK) and P. G. GLOCKNER (CALGARY)

The problem of collapse by ponding of air-supported spherical membranes subjected to a central load is considered. Linearly elastic and two-way membrane action is assumed. The equilibrium of the spherical cap is analyzed and the equations for the determination of the critical central weight for the onset of collapse are derived. Numerical solutions are obtained for a range of internal pressures, elastic moduli, height/span ratios and radii of curvature. Results from the present study for large elastic moduli are compared with previously obtained experimental data and theoretical predictions [8, 11].

1. Introduction

Pneumatic membrane structures have become quite common during the last decade for providing low cost temporary enclosures for exhibitions and construction sites as well as for permanent coverings for warehouses, greenhouses and athletic facilities [1–7] (1). However, the design methods for these air-supported structures are still in a state of development. One peculiar aspect of these membrane structures is the possibility of collapse by accumulation of rain, ice or snow on their surfaces. Failure in this mode has been reported in several cases and has also been observed experimentally [8, 9].

Investigations of ponding collapse of cylindrical and spherical pneumatic membrane structures were carried out recently [8–13]. More specifically, a theory for ponding instability of spherical membranes was discussed in [8, 11] where it was assumed that the membrane material is inextensional and the membrane acts only in the meridional direction in the ponding region and in part of the rest of the membrane.

In the present work the problem of ponding collapse of air-supported spherical caps subjected to a central weight is considered with the assumptions that the membrane is linearly elastic and acts in both directions throughout. Equilibrium in the ponding region and in the rest of the membrane is considered in obtaining a solution from which the critical central weight causing the onset of collapse is

(*) The results presented here were obtained in the course of research sponsored by the Natural Sciences and Engineering Research Council of Canada, Grant No. A-2736.

(1) Numbers in square brackets refer to publications listed under References.

deduced by maximization of a two-variable function subjected to an integral equation constraint. The extremization problem is solved by a numerical iteration scheme and the magnitude of the critical central weight for a range of internal pressures, elastic moduli and geometric parameters obtained and presented in graphical form.

2. Mathematical model

Figure 1 shows a cross-section through a weightless spherical membrane subjected to an internal pressure, p, a central concentrated load, W, and the weigh of a ponding fluid of weight density, ρ, which is accumulating in the central depression caused by the deflection. The undeformed shape of the membrane is a perfect spherical cap of radius, R. The inflated shape, in the absence of a central weight and ponding fluid, is also a spherical cap as is shown in Figure 1. It is assumed that the membrane is elastic and acts in both directions throughout.

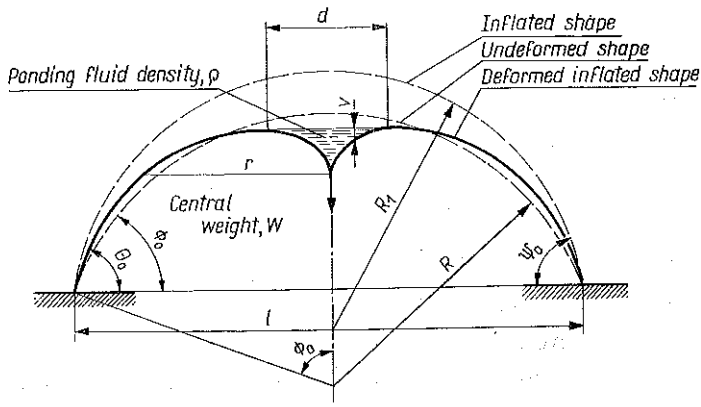

Fig. 1. Cross-section of spherical membrane with central weight and ponding fluid.

In analyzing the equilibrium of the membrane, two regions are considered, one in which the ponding fluid is accumulating and a second one outside the ponding region. If the pond and the deflections of the membrane are small, a linear membrane theory for this region may be employed. As a result, the equation of equilibrium normal to the membrane becomes (see for instance, [14])

$$T\frac{d}{dr}\left(r\frac{dv}{dr}\right)=(p-\rho v)\,r\,, \qquad 0\leqslant r\leqslant\frac{d}{2}\,, \tag{1}$$

where r is the radial distance from the axis of symmetry, v denotes vertical displacement, p is the internal pressure and T is the constant membrane tension per unit length. In Eq. (1), d is the pond diameter which itself is an unknown.

The deflections must satisfy the following boundary conditions:

$$v=0, \quad \text{at} \quad r=\frac{d}{2} \tag{2}$$

$$\frac{dv}{dr}=0, \quad \text{at} \quad r=\frac{d}{2}, \tag{3}$$

$$W=-2\pi Tr\frac{dv}{dr} \quad \text{as} \quad r\to 0. \tag{4}$$

Equation (3) states that the slope of the membrane at the edge of the pond must be zero and Eq. (4) is the condition of equilibrium at the concentrated load, W. The general solution to Eq. (1) is given by

$$v=AJ_0(kr)+BY_0(kr)+p/\rho, \tag{5}$$

where

$$k^2=\frac{\rho}{T}. \tag{6}$$

In Eq. (5), J_0 and Y_0 are the zero order Bessel functions of first and second kinds, and A and B are constant parameters.

Employing boundary conditions (2) and (3), the values of the constants A and B are determined. The equilibrium condition (4) then yields

$$W=\frac{\pi pd}{k}J_1\left(k\frac{d}{2}\right), \tag{7}$$

where J_1 is the Bessel function of the first kind of order one. Equation (7) relates the magnitude of the central weight to the internal pressure, the pond diameter, the fluid density and the membrane tension. The maximum of the right-hand side of Eq. (7) provides an upper limit for the central weight which is the threshold of instability. However, for a given internal pressure and fluid density, the pond diameter and the membrane tension are related through equilibrium of the rest of the membrane.

Noting that at the edge of the pond the membrane is horizontal, the equation of overall vertical equilibrium of the cap above radius r becomes

$$2\pi rT\sin\theta=\pi\left(r^2-\frac{d^2}{4}\right)p, \tag{8}$$

where θ is the slope with the horizontal (see Figure 1) from which one obtains

$$\sin\theta=\left(r-\frac{d^2}{4r}\right)\left(\frac{p}{2T}\right). \tag{9}$$

At the support, Eq. (9) becomes

$$\sin\theta_0=\left(l-\frac{d^2}{l}\right)\left(\frac{p}{4T}\right), \tag{10}$$

where l is the span of structure.

In the absence of a central weight and ponding fluid, d becomes zero in which case it follows from Eqs. (9) and (10) that the inflated shape is a sphere and the slope at the base is given by ψ_0 which is also shown in Figure 1. For negligible extensibility of the membrane, (i.e. very small internal pressure or very high modulus of elasticity) the undeformed shape is recovered. The undeformed angle at the base is given by φ_0, as shown in Figure 1. Noting that $l=2R\sin\varphi_0$, Eq. (10) reduces to the well-known relation

$$T_0=\frac{pR}{2}. \tag{11}$$

For the inflated extensible membrane, in the absence of a central weight and ponding fluid, the expression for tension becomes

$$T_1=\frac{pR_1}{2}, \tag{12}$$

where the radius R_1 must also be determined. In the presence of a central weight and a ponding fluid, the magnitude of the membrane tension is not directly available; however, it is less than the limit given by Eq. (11) and is a function of the magnitude of the central weight and the pond size. Furthermore, variation of the membrane tension results in a change of arc length due to the extensibility of the material which is assumed to be Hookean with Poisson ratio $\nu=0$. The change in length, Δs, is assumed to be related to the membrane tension and the original length, s, by the following expression

$$T=E\frac{\Delta s}{s}, \tag{13}$$

where E is the elastic modulus in Newtons/m. Assuming the membrane tension in the deformed state to be T, the length of a meridional arc from the axis of symmetry to the base becomes

$$S=R\varphi_0\left(1+\frac{T}{E}\right). \tag{14}$$

On the other hand, within the limits of linear theory

$$S=\frac{d}{2}+s, \tag{15}$$

where s is the length of the meridional arc outside the ponding region in the deformed state, i.e.

$$s=\int_{d/2}^{l/2}\frac{dr}{\cos\theta}. \tag{16}$$

Using Eqs. (9), (14) and (16) in Eq. (15), one obtains

$$\frac{d}{2}+\int_{d/2}^{l/2}\{1-[(p/2T)(r-d^2/4r)]^2\}^{-1/2}\,dr=R\varphi_0\left(1+\frac{T}{E}\right). \tag{17}$$

Eq. (17) relates the membrane tension to the pond diameter.

The problem then is to find the maximum of Eq. (7) subject to the constraint given by Eq. (17). Before attempting to solve this problem, it is advantageous to introduce dimensionless quantities. Considering the radius, R, as a length scale, the following dimensionless variables are introduced, which are designated by a bar above the symbols,

$$\begin{aligned} &\bar{d}=d/R, \qquad \bar{l}=l/R=2\sin\varphi_0,\\ &\bar{p}=p/\rho R, \quad \bar{T}=T/\rho R^2, \quad \bar{T}_0=T_0/\rho R^2=\bar{p}/2, \end{aligned} \tag{18}$$

and

$$\bar{W}=W/\pi p R^2, \qquad \bar{E}=E/\rho R^2. \tag{19}$$

Employing these dimensionless quantities in Eqs. (7) and (17), one finds

$$\bar{W}=\bar{d}\bar{T}^{1/2}J_1(\bar{d}/2\bar{T}^{1/2}), \tag{20}$$

$$\frac{\bar{d}}{2}+\int_{\bar{d}/2}^{\bar{l}/2}\{1-[(\bar{p}/2\bar{T})(r-\bar{d}^2/4r)]^2\}^{-1/2}\,dr=\varphi_0(1+\bar{T}/\bar{E}). \tag{21}$$

The dimensionless critical central weight is now given as the maximum of Eq. (20) with respect to $\bar{d}$, with $\bar{T}$ given implicitly in terms of $\bar{d}$ by Eq. (21). Numerical solution of this general extremization problem is discussed in the next section. Here, a special limiting case of interest is briefly described. For small values of the pond size, and almost inextensible membranes (i.e. $\bar{E}$ large), the approximate value of the dimensionless tension, as found from Eq. (21) becomes

$$\bar{T}=\bar{p}/2, \tag{22}$$

which corresponds to the underformed state of the spherical membrane. When the approximation given by Eq. (22) is employed, Eq. (20) provides $\bar{W}$ explicitly in terms of $\bar{d}$. The maximum of $\bar{W}$ may then be found by simple evaluation of its first derivative with respect to $\bar{d}$. The critical dimensionless pond diameter for this approximation becomes

$$\bar{d}=2\beta_0\bar{T}^{1/2}=\beta_0(2\bar{p})^{1/2}, \tag{23}$$

where

$$\beta_0=2.4048, \tag{24}$$

corresponds to the position of the first zero of the Bessel function of zero order, (i.e. $J_0(\beta_0)=0$). The corresponding critical value of the dimensionless critical central weight becomes

$$\bar{W}=\beta_0 J_1(\beta_0)\bar{p}=1.248\,\bar{p}. \tag{25}$$

In dimensional form, this critical central weight is given by

$$W=3.922\,p^2\,R/\rho\,. \tag{26}$$

It is of interest to note that the approximate critical central weight given by Eqs. (25) or (26) is independent of the span l (or undeformed ground angle φ_0), the elastic modulus of the membrane, E, and is solely determined by the radius, the internal pressure and the fluid density. Therefore, Eqs. (25) and (26) provide a relatively simple rough estimate for the critical central weight for a large class of membrane shapes and conditions. Furthermore, as shall be seen from the results presented in the next section, the estimates given by Eqs. (25) and (26) are remarkably accurate within a certain range of the parameters.

3. Numerical solutions and results

For given internal pressure, $\bar{p}$, elastic modulus, $\bar{E}$, and undeformed membrane shape, φ_0, finding the maximum of $\bar{W}$, as given by Eq. (20), with respect to $\bar{d}$ and $\bar{T}$, and subjected to the constraint given by Eq. (21), is clearly a well posed problem. However, due to the complexity of the constraint, an analytical solution is intractable and the maximization is carried out by an iteration technique. A computer programme was developed which iterates for various values of the dimensionless pond diameter, $\bar{d}$, in finding the maximum of $\bar{W}$. The value of $\bar{T}$, corresponding to each value of $\bar{d}$, is found by satisfying Eq. (21) through another iteration scheme.

For various underformed shapes of the spherical cap, and several values of dimensionless internal pressure and elastic moduli, the magnitudes of the dimensionless critical central weight are obtained and the results given in Figures 2–4. Figure 2 shows the variation of $\bar{W}$ with dimensionless internal pressure, $\bar{p}$, for several values of undeformed ground angles, φ_0, for a large value of dimensionless elastic modulus. It is observed that the dimensionless critical weight increases rapidly with an increase in $\bar{p}$ and decreases slightly with a decrease of φ_0. The approximate estimate of $\bar{W}$, as provided by Eq. (25) is also shown in Figure 2 and is observed to give an upper bound for the critical central weight. Furthermore, the estimate given by Eq. (25) is remarkably accurate for $\varphi_0 \geqslant 45°$ and for the range of internal pressures considered. Another observation from Figure 2 is that for $\varphi_0 \geqslant 30°$ $\bar{W}$ does not vary appreciably with change of shape of the spherical cap for $\bar{p}$ lower than 0.003.

In Figure 3, the variation of $\bar{W}$ with $\bar{p}$ for several values of φ_0 and for $\bar{E}=0.05$ are shown. The prediction by means of Eq. (25) is also given by a dashed line. The general form of the curves for critical central weights for the elastic membrane is quite similar to the corresponding form for the inextensible membrane, given in Figure 2. However, $\bar{W}$ for the elastic membranes are lower than those for the inextensible membranes of the same shape and subjected to the same internal pressure. Furthermore, the variation in $\bar{W}$ with φ_0 is much more substantial for the elastic membrane (with $\bar{E}=0.05$) than for the inextensible membrane. Eq. (25) still provides very good estimates for $\bar{W}$, for $\varphi_0 \geqslant 75°$ even for relatively small values of the elastic modulus.

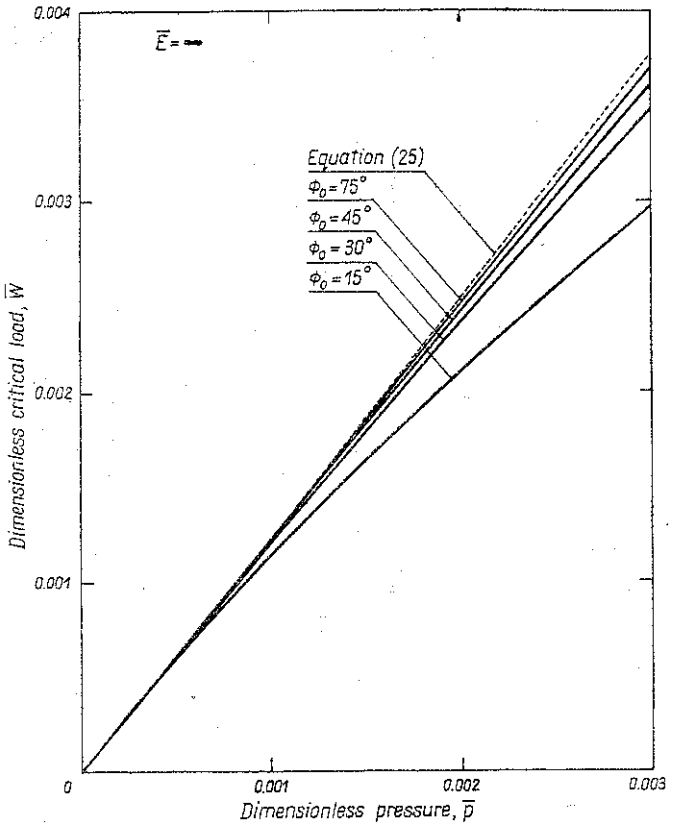

FIG. 2. Variations of dimensionless critical central weight with dimensionless internal pressure for different underformed shapes for large values of $\bar{E}$

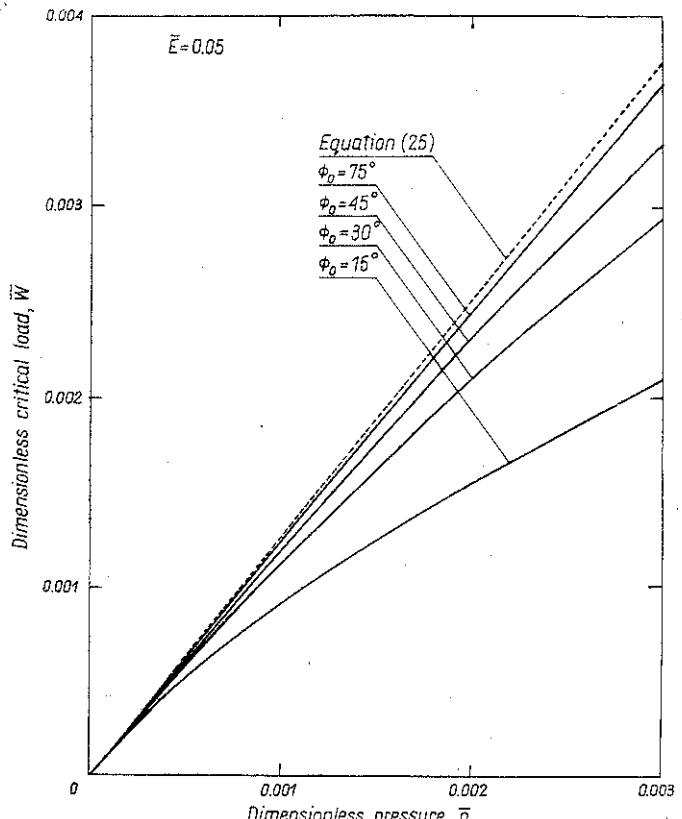

FIG. 3. Variations of dimensionless critical central weight with dimensionless internal pressure for different underformed ground angles for $\bar{E}=0.05$

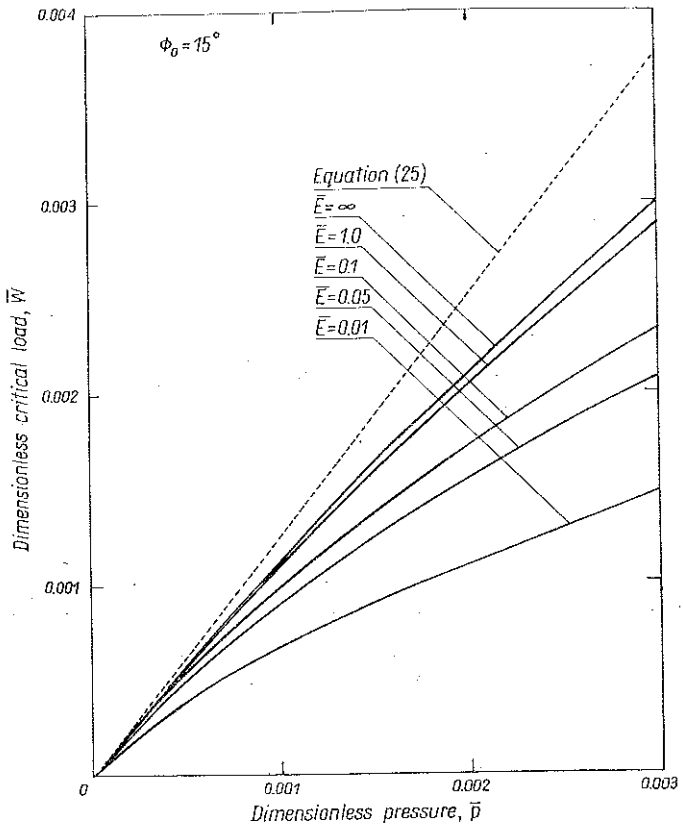

FIG. 4. Variations of dimensionless critical central weight with dimensionless internal pressure for several values of elastic moduli for $\varphi_0=15°$.

The effect of variation of $\bar{E}$ on $\bar{W}$, for various values of $\bar{p}$, are given in Figure 4. These results are purposely shown for a very shallow spherical membrane ($\varphi_0=15°$) for which the effects of extensibility on $\bar{W}$ are most severe. We note that as the elastic modulus decreases (i.e. the membrane becomes more extensible), $\bar{W}$ also decreases rapidly for such a relatively shallow spherical membrane. Results for other values of φ_0 show that the effect of extensibility on $\bar{W}$ becomes smaller with increasing φ_0 and for $\varphi_0 \geqslant 75°$, this effect becomes negligible so that Eq. (25) can be used to predict $\bar{W}$ with sufficient accuracy for values of $\bar{E}$ of the order of 0.05.

It should be noted here that the case of $\bar{E}=\infty$, shown in Figures 2, 4 and in the rest of the figures, is practically reached for $\bar{E} \geqslant 5$ for the range of shapes and pressures considered. For relatively large values of φ_0 (i.e. $\varphi_0 \geqslant 45°$) the inextensibility limit is reached for $\bar{E} > 1$.

In Figure 5, the dimensionless critical pond diameter, $\bar{d}$, is plotted against $\bar{p}$, for several shapes of inextensible membranes by solid lines, and for various elastic moduli for an angle of $\varphi_0=15°$ by broken lines. The prediction from Eq. (23) is also shown. It is observed that $\bar{d}$ is below 0.2 in the range of parameters considered, which justifies the use of the linearized Eq. (1) and Eq. (15). Furthermore, it is

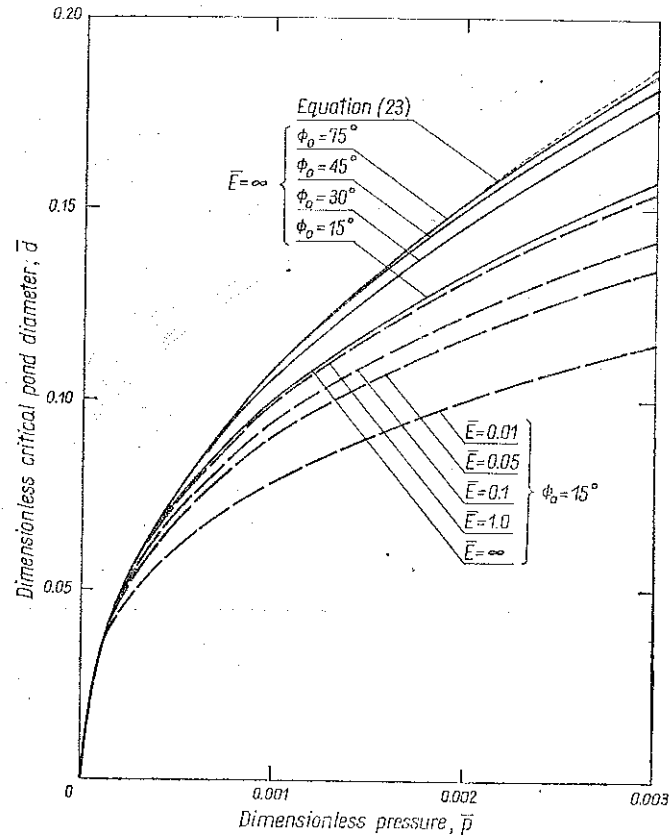

FIG. 5. Variations of dimensionless pond diameter with dimensionless internal pressure for several values of undeformed ground angles for $\bar{E}=\infty$ and for several values of elasctic moduli for $\varphi_0=15°$.

seen that $\bar{d}$ increases with an increase in internal pressure and an increase in φ_0, while it decreases with a decrease in $\bar{E}$. The curves for various values of $\bar{E}$, shown in Figure 5, correspond to quite a shallow spherical cap of $\varphi_0=15°$. For higher values of φ_0, the effects of extensibility in reducing $\bar{d}$ is less significant. From Figure 5, it is also observed that for $\varphi_0 \geqslant 75°$, the predicions from Eq. (23) are extremely accurate in the range of the internal pressures considered.

Although, the values of the critical central weight and pond diameter for different magntiudes of the internal pressure and elasticity of membrane material for various underformed shapes of the spherical air supported membranes could be found from the nondimensionalized Figures 2–5, it is useful to consider a few examples of practical interest in dimensional forms. The critical central weight for the onset of instability are evaluated for inextensible as well as elastic spherical membranes of various shapes and spans subjected to variable internal pressure and the results are plotted in Figures 6–11. The ponding fluid is assumed to be rain water of a weight density of 10^4 Newtons/m^3 throughout. In Figure 6, W is plotted versus p for an inextensible spherical membrane of $\varphi_0=30°$ for several values of radius from 10 to 50 meters.

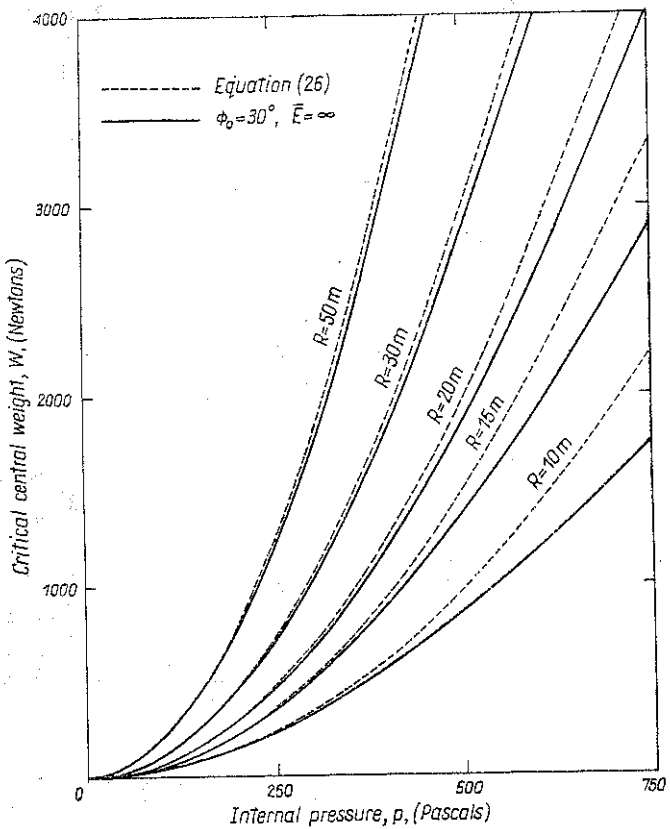

FIG. 6. Comparison of the values of the critical central weight of an inextensible spherical membrane of underformed ground angle of 30° with the predictions of Eq. (26) for several values of underformed radius and internal pressures.

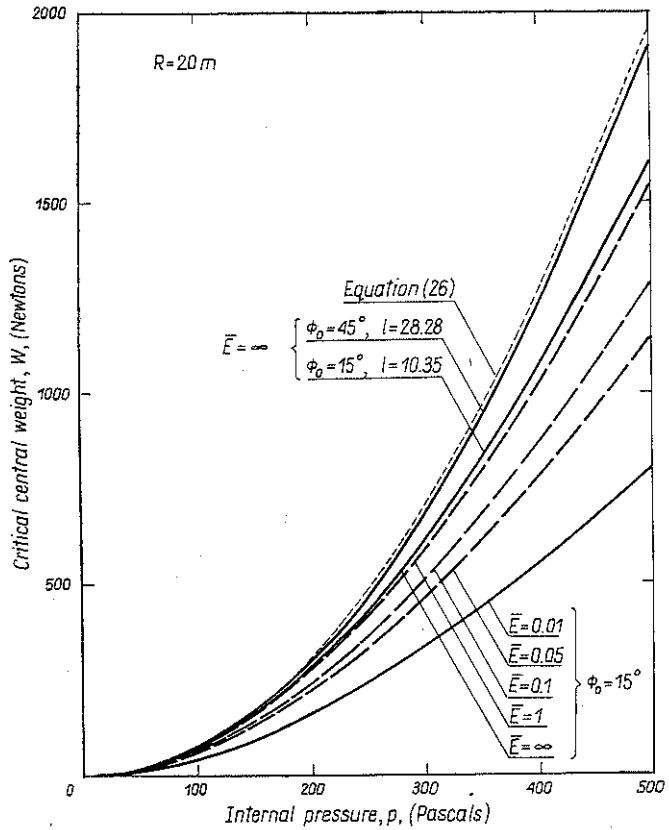

FIG. 7. Effects of shape and extensibility on the critical central weight of a spherical membrane of undeformed radius 20 meter subjected to different magnitudes of internal pressure.

The corresponding predictions of Eq. (26) are also shown in this figure by dashed lines. It is observed that W increases rapidly with an increase in p and also increases with an increase in R. Eq. (26) provides an upper bound for W for each given radius which is also independent of the shape of the spherical cap. Due to the fact that the curves of W vs. p for $\varphi_0 > 30°$ will fall between the corresponding solid and dashed lines on Figure 6, it is concluded that Eq. (26) yields relatively accurate estimates for W for an inextensible spherical membrane with $R > 30$ m and $\varphi_0 \geqslant 30°$, $p \leqslant 600$ Pa. For larger φ_0 the range of accuracy extends to lower values of R.

The effects of variations in shape and extensibility on the magnitude of the critical central weight for a spherical membrane with $R=20$ meters are shown in Figure 7. It is observed that W increases with an increase in φ_0 when R is kept fixed and it decreases with a decrease in E. The effect of extensibility in reducing the magnitude of the critical central weight is accentuated for small values of φ_0.

For the fixed values of internal pressures of 150 and 300 Pascals, the variations of W for a spherical cap with $\varphi_0 = 15°$ with its radius are shown in Figure 8. It is observed that W increases almost linearly with membrane radius and the rate of increase is much more rapid for $p=300$ Pascals as compared with $p=150$ Pascals.

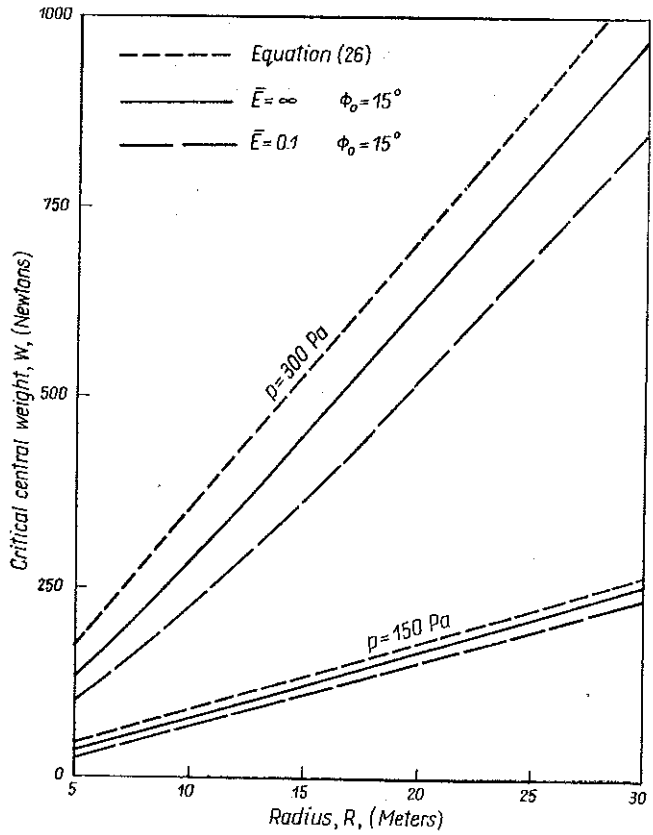

FIG. 8. Variations of the critical central weight with underformed radius for different values of internal pressure and elastic moduli for a spherical cap of underformed angle of 15°.

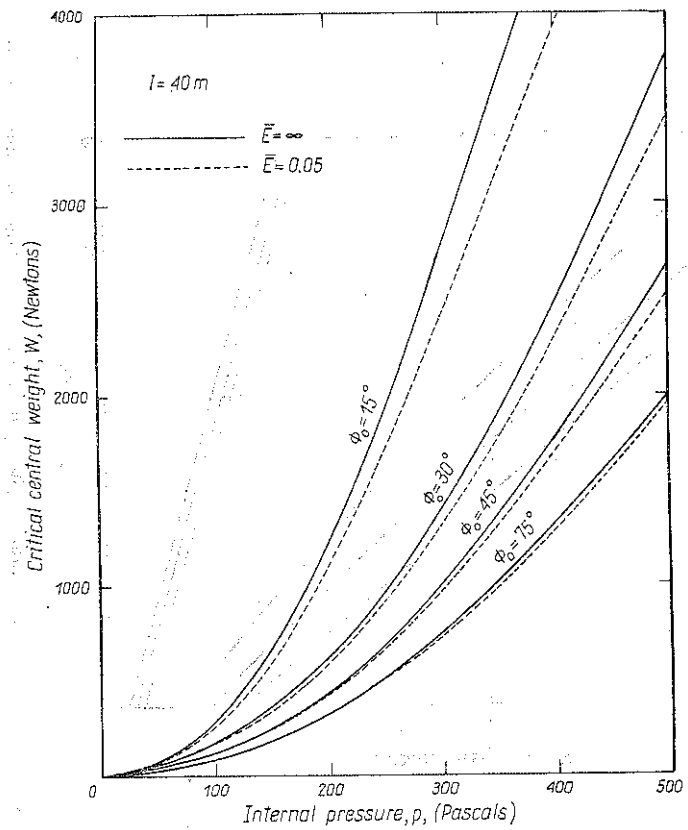

FIG. 9. Effects of shape and extensibility on the critical central weight of a spherical membrane spanning a diameters of 40 meters and subjected to a range of values of internal pressure.

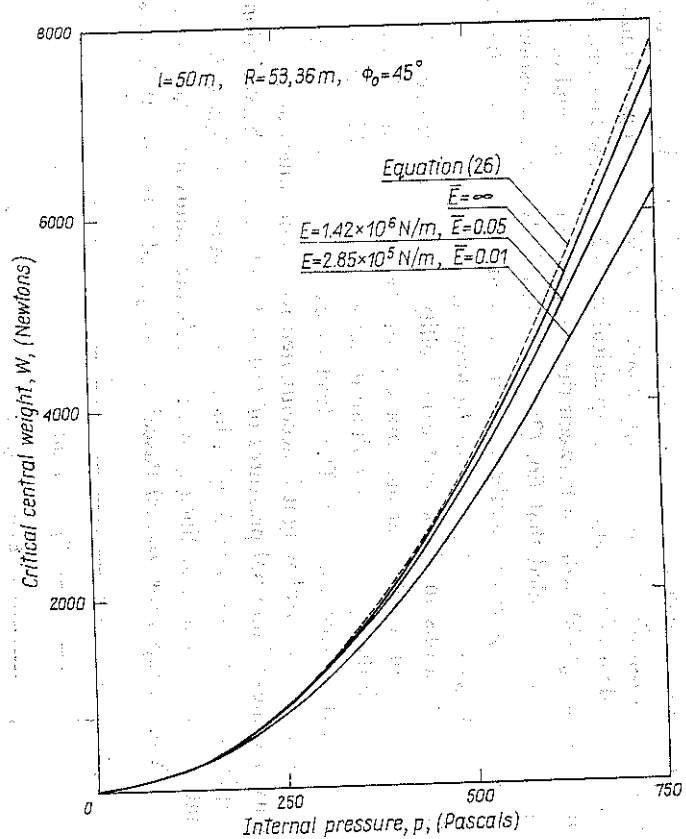

FIG. 10. Variations of the critical central weight of a spherical cap of undeformed ground angle of 45° spanning a diameter of 50 meters with internal pressure for several values of elastic moduli.

For a fixed span of $l=40$ meters, the variation of W with internal pressure for several values of φ_0 are shown in Figure 9. It is observed that W increases with a decrease in φ_0 and increases with an increase in p. This rate of increase is much faster for the shallower spherical membrane spanning the same diameter. The critical central weight of the elastic membrane is lower than that of the corresponding inextensible one and the difference is more substantial for relatively flat membranes as compared with the steeper ones.

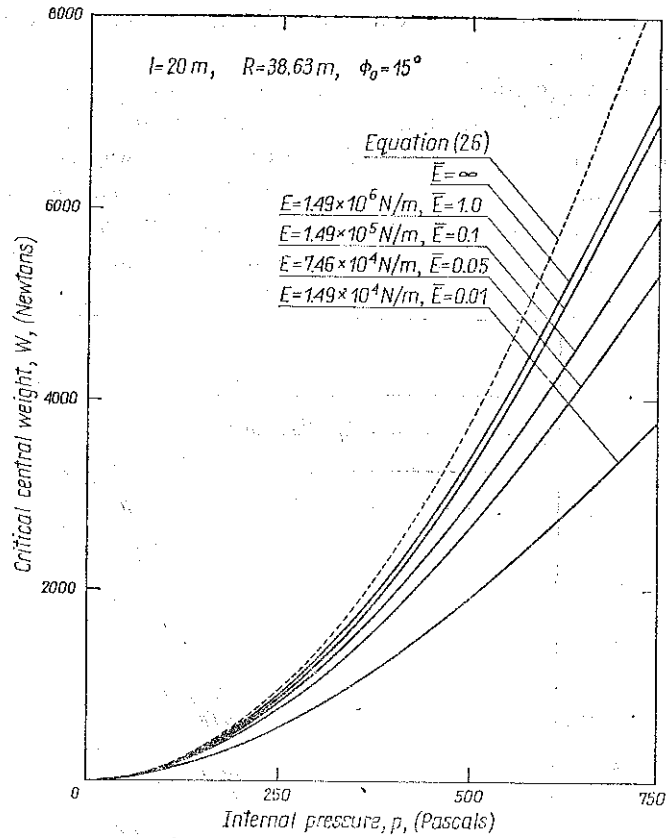

FIG. 11. Variations of the critical central weight of a spherical cap of undeformed ground angle of 15° spanning a diameter of 20 meters with internal pressure for several values of elastic moduli.

For a span of 50 meters and $\varphi_0=45°$, the variation of W with p for several values of E are shown in Figure 10. The reducing effect of extensibility on the magnitude of the critical central weight can be clearly observed from this figure.

Figure 11 shows the variation of W with internal pressure for several values of E for spherical caps with $\varphi_0=15°$ spanning a diameter of 20 meters. The observations from this figure is similar to those of Figure 10, except that the effect of extensibility in reducing the magnitude of the critical central weight is now quite profound due to the relatively flat shape of the membrane.

4. Comparison with previous works

In [8, 11] the problem of collapse by ponding of inextensible spherical membranes was treated where it was assumed that the membrane act only in the meridional direction in the pond region and in part of the membrane outside that region. The present work considers elasticity of the membrane and assumes two-way action throughout. Even for large values of the elastic modulus, where the limit of inextensibility is approached, the two-way action is still preserved. It is therefore of interest to compare the predicions of the present study with the theoretical and experimental results given in [8, 11].

The theoretical predictions of [8] for variations of the critical central weight with internal pressure for spherical membranes of 10 and 20 meters radii are reproduced in Figure 12. As a consequence of the assumed one-way action, the critical central weight becomes independent of the shape (l or φ_0). The predictions of the present two-way membrane action model for the limit of a large elastic modulus for the underformed grou nd angles of 60° and 15° together with the results of Eq. (26)

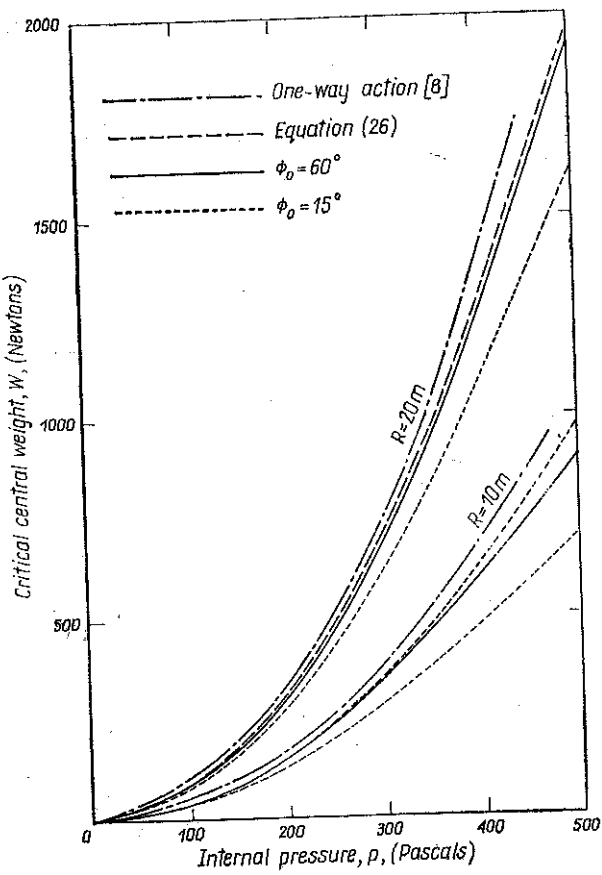

Fig. 12. Comparison of the predicted critical central weight with the results of the partially one-way action model of [8].

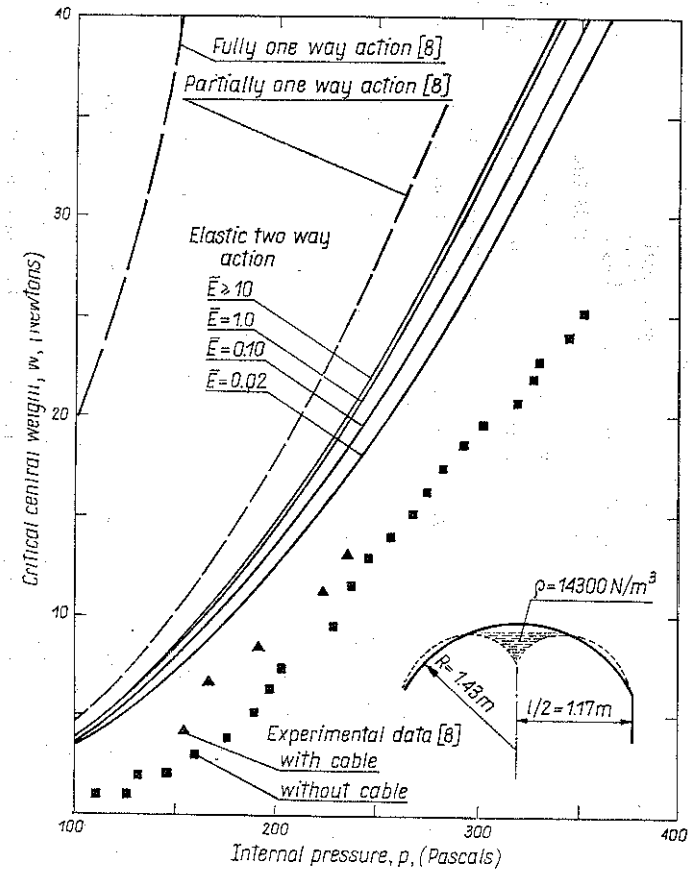

FIG 13. Comparison of the predicted critical central weight with the results of completely one-way action model of [8].

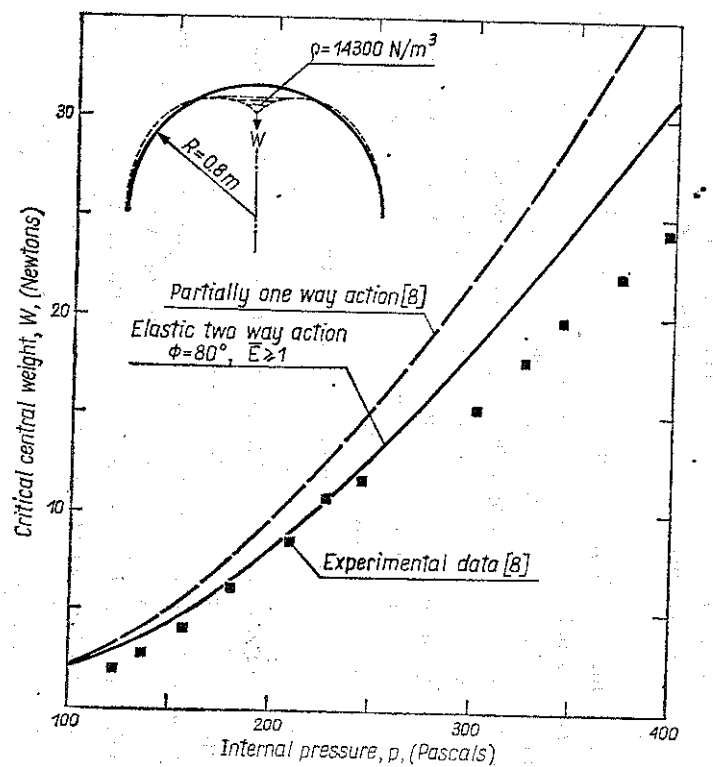

FIG. 14. Comparisons of the predictions of the present model with the theoretical results and experimental data of [8].

are also shown in Figure 12. It is observed that the present two-way membrane action model predicts lower values for W and the difference increases with a decreaase in φ_0.

The experimental data for the critical central weight under various internal pressure as reported in [8] are shown in Figures 13 and 14. The ponding medium was a fine quality. Ottawa sand with a weight density of 14.300 N/m^3. The results shown in Figure 13 are for a spherical cap of radius 1.43 meters and a span of 2.34 meters. The predicions of the one-way membrane action model of [8] are also shown in this figure by the dashed curve. The results of the present two-way elastic membrane action model for various values of elastic moduli are plotted in Figure 13 by the solid curves. It is observed that the present model predicts lower values for the critical central weight as compared with the theoretical results of [8]. Although the present predictions for W are closer to the experimental data, as is observed from Figure 13, discrepancies ranging from 4 to 12 Newtons do still exist.

In [8], it was suggested that the membrane used in the experiment was probably imperfect and allowing a two percent increase in the length of a meridional arc length, it was possible to match the theory with the experimental data. Such adjustment could also be carried out for the present theory with a much lower value for the imperfection. Another factor which could be the reason for part of the observed discrepancy is the effect of the self-weight of the membrane which according to [8] was 8 N/m^2 and near the apex reaches an average of 14 N/m^2. Noting that the surface area of the model was more than 4 m^2, the weight of the membrane becomes several times the discrepancies observed.

Figure 14 shows the comparisons of the predicion of the present model with the theoretical and experimental results of [8] for a semi-spherical membrane of radius 0.8 meters. The predicion of the present model shown in Figure 14 is for $\varphi_0=80°$, since for larger values of φ_0, the deformed ground angle exceeds the value of 90° which produces some difficulties in the convergence of the numerical extremization scheme. The agreements between the present theory and the experimental data of [8] is quite reasonable for the lower values of internal pressure, however, noticeable discrepancies between the theory and experiment still exist for the higher values of p. As noted before, the differences between the theory and experiment could be partially due to the self-weight or the imperfections in the shapes of the experimental spherical caps.

5. Conclusions

Based on the results obtained in the present study the following conclusions may be drawn:

i) The critical central weight, W, increases with increase in p, R and φ_0.

ii) The rate of increase of W with p increases with radius.

iii) For fixed values of span, the critical central load decreases with an increase of φ_0. In other words, flat spherical caps are more stable than steeper ones.

iv) The critical central weight for an elastic membrane is less than that of the corresponding inextensible one, and the value of W decreases with a decrease in E. Furthermore, the reduction in W is more pronounced at smaller values of φ_0.

v) For a given pressure and radius, the approximation given by Eq. (26) provides an upper bound for the critical central weight for arbitrary values of span (or φ_0) and E. This equation provides good estimates for the relatively inextensible membranes with moderate to large values of φ_0. When E decreases, Eq. (26) gives reasonable estimates only for small to moderate values of φ_0.

vi) The critical pond diameter increases with increase of p, φ_0 and E.

REFERENCES

1. P. S, BULSON, *Design principles of pneumatic structures*, The Structural Engineer, **51**, 209–215, 1953.
2. W. W. BIRD, *The development of pneumatic structures, past, present and future*, IASS 1st Int. Colloquium on Pneumatic-Structures, Stuttgart, May 1967.
3. D. H. GEIGER, *U. S. pavillion at Expo 70 features air supported cable roof*, Civil Engineering, ASCE, 48–50, March 1970.
4. D. H. GEIGER, *Developments in incombustible fabrics and low profile air structures*, Int. Conf. on Practical Applications of Air-Supported Structures, Las Vegas, pp. 211, October 1974.
5. R. A. KINNIUS, *The modern concept of air-supported structures*, CIB/IASS Int. Symposium on Air Supported Structures, Venice June 1977, 43–49.
6. P. G. GLOCKNER and D. J. MALCOLM, *The use of inflatables in agriculture and the exploration industry*, CIB/IASS Int. Symposium on Air-Supported Structures, Venice 377–407, June 1977.
7. Y. YOKO, H. MATSUNAGA and Y. YOKOYAMA, *On the behaviour of Wrinkled regions of pneumatic membrane in the form of a surface of revolution under symmetric loading*, Proc. IASS Pacific Symposium (Pt. II), Tension Structures and Space Frames, Tokyo and Kyoto, 449–460, 1971.
8. D. J. MALCOLM and P. G. GLOCKNER, *Collapse by ponding of air-supported spherical caps*, Department of mechanical Engineering, Report No. 174, The University of Calgary, September 1980.
9. D. J. MALCOLM, *Ponding instability of air-supported cylinders — some experimental results*, Department of mechanical Enginnering, Report No. 137, The University of Calgary, December 1978.
10. D. J. MALCOLM and P. G. GLOCKNER, *Collapse by ponding of air-supported membranes*, Proc. ASCE **104**, No. ST9, Proc. Paper 14002, 1525–1532, September 1978.
11. D. J. MALCOLM and P. G. GLOCKNER, *Ponding stability of an air-supported spherical membrane*, Proc. Seventh Can. Congress Appl. Mech., CANCAM '79, Sherbrocke, P. Q., **1**, 135–136, May 27—June 1, 1979.
12. P. G. GLOCKNER and D. J. MALCOLM, *Some problems in using cable-reinforced inflatables in greenhousing*, Department of Mechanical Engineering, Report No. 161, The University of Calgary April 1980.
13. G. AHMADI and P. G. GLOCKNER, *Ponding instability of inflated imperfect cylindrical membranes*, ASCE J. Struct. Div. [in press].
14. T. V. KÁRMÁN and M. A. BIOT, *Mathematical methods in engineering*, 315–316, McGraw-Hill New York 1940.

STRESZCZENIE

NIESTATECZNOŚĆ PNEUMATYCZNYCH, SFERYCZNYCH MEMBRAN SPRĘŻYSTYCH

Rozważono problem zniszczenia centralnie obciążonych membran sferycznych podpartych na poduszce powietrznej, spowodowane przez powstanie lokalnych wybrzuszeń (przeskoków). Założono, że obustronnie pracująca membrana jest liniowo sprężysta. Przeanalizowano równowagę sferycznej powłoki i wyprowadzono równania pozwalające określić krytyczną wartość centralnej siły obciążającej prowadzącej do zniszczenia. Otrzymano rozwiązania w postaci numerycznej w pewnym zakresie ciśnień wewnętrznych, modułów sprężystości, wyniosłości powłoki i jej promienia krzywizny. Wyniki analizy przy dużych wartościach modułów sprężystości porównano z uzyskanymi wcześniej danymi doświadczalnymi i przewidywaniami teoretycznymi [8, 11].

Резюме

НЕУСТОЙЧИВОСТЬ ПНЕВМАТИЧЕСКИХ СФЕРИЧЕСКИХ УПРУГИХ МЕМБРАН

Рассмотрена проблема разрушения центрально нагруженных, сферических мембран, подпертых на воздушной подушке, вызванная возникновением локальных выпучиваний (перескоков). Предположено, что обусторонне работающая мембрана является линейно упругой. Проанализировано равновесие сферической оболочки и выведены управнения, позволяющие определить критическое значение центральной нагружающей силы, приводящей к разрушению. Получены решения в численном виде в некотором интервале внешних давлений, модулей упругости степени пологости оболочки и ее радиуса кривизны. Результаты анализа при больших значениях модулей упругости, сравнены с полученными раньше экспериментальными данными и теоретическими предсказываниями [8, 11]

DEPARTMENT OF MECHANICAL AND INDUSTRIAL ENGINEERING
CLARKSON COLLEGE, POTSDAM, NEW YORK, USA
and
DEPARTMENT OF MECHANICAL ENGINEERING
THE UNIVERSITY OF CALGARY, ALBERTA, CANADA

Received December 14, 1982.